

This article was downloaded by: [University of Haifa Library]

On: 16 August 2012, At: 12:43

Publisher: Taylor & Francis

Informa Ltd Registered in England and Wales Registered Number: 1072954

Registered office: Mortimer House, 37-41 Mortimer Street, London W1T 3JH, UK



Molecular Crystals and Liquid Crystals Science and Technology. Section A. Molecular Crystals and Liquid Crystals

Publication details, including instructions for authors and subscription information:

<http://www.tandfonline.com/loi/gmcl19>

Long-Time Behavior of the Azimuthal Anchoring Strength and Easy Axis Gliding of Nematic Liquid Crystal

D. N. Stoenescu^{a b}, I. Dozov^{a c} & Ph. Martinot-Lagarde^a

^a Laboratoire de Physique des Solides, Université Paris-Sud, 91405, Orsay, France

^b INCDFM - Măgurele, POBox MG7, 76900, Bucharest, Romania

^c Institute of Solid State Physics, 72 blvd. Tsarigradsko Chaussee, 1784, Sofia, Bulgaria

Version of record first published: 24 Sep 2006

To cite this article: D. N. Stoenescu, I. Dozov & Ph. Martinot-Lagarde (2000): Long-Time Behavior of the Azimuthal Anchoring Strength and Easy Axis Gliding of Nematic Liquid Crystal, *Molecular Crystals and Liquid Crystals Science and Technology. Section A. Molecular Crystals and Liquid Crystals*, 351:1, 427-434

To link to this article: <http://dx.doi.org/10.1080/10587250008023294>

PLEASE SCROLL DOWN FOR ARTICLE

Full terms and conditions of use: <http://www.tandfonline.com/page/terms-and-conditions>

This article may be used for research, teaching, and private study purposes. Any substantial or systematic reproduction, redistribution, reselling, loan, sub-licensing, systematic supply, or distribution in any form to anyone is expressly forbidden.

The publisher does not give any warranty express or implied or make any representation that the contents will be complete or accurate or up to date. The accuracy of any instructions, formulae, and drug doses should be independently verified with primary sources. The publisher shall not be liable for any loss, actions, claims, proceedings, demand, or costs or damages whatsoever or howsoever caused arising directly or indirectly in connection with or arising out of the use of this material.

Long-Time Behavior of the Azimuthal Anchoring Strength and Easy Axis Gliding of Nematic Liquid Crystal

D.N. STOENESCU^{ab}, I. DOZOV^{ac} and PH. MARTINOT-LAGARDE^a

^a*Laboratoire de Physique des Solides, Université Paris-Sud, 91405 Orsay, France,*

^b*INCDFM – Măgurele, POBox MG7, 76900 Bucharest, Romania and* ^c*Institute of Solid State Physics, 72 blvd. Tsarigradsko Chaussee, 1784 Sofia, Bulgaria*

We measure the azimuthal anchoring strength and easy axis gliding of the nematic 5CB on weakly anisotropic substrate. We study the anchoring evolution at a time scale ranging from a few minutes up to a few months. We separate approximately the elastic and the viscous response and we obtain the gliding velocity as a function of the applied torque. We discuss the observed gliding times and nonlinear gliding viscosity.

Keywords: anchoring strength; azimuthal anchoring; anchoring memory; nematic; anchoring gliding

INTRODUCTION

Usually, the anisotropic interaction with a solid surface induces an orientation of the liquid crystal molecules. This phenomenon, known as alignment or anchoring, orients the surface director \mathbf{n}_s parallel to some "easy" axis \mathbf{n}_e , a fixed direction defined by the surface anisotropy. When a torque Γ_b is applied, \mathbf{n}_s deviates from \mathbf{n}_e , giving rise to an opposite anchoring torque $\Gamma_s(\mathbf{n}_s - \mathbf{n}_e)$. This can be described by a surface anchoring energy $W_s(\mathbf{n}_s - \mathbf{n}_e)$, minimized for $\mathbf{n}_s = \mathbf{n}_e$. Usually, $W_s(\mathbf{n}_s - \mathbf{n}_e)$ is highly anisotropic and much stronger for zenithal deviation than for azimuthal one. In the following, we are interested only in the azimuthal anchoring and we apply only azimuthal torques. We then suppose that \mathbf{n}_s and \mathbf{n}_e lie in the plane of the substrate and are defined by their azimuthal angles, respectively φ_s and φ_e . In Rapini-Papoular approximation^[1] we expect

$$W_s(\varphi_s - \varphi_e) = \frac{1}{2} A \sin^2(\varphi_s - \varphi_e) \quad (1)$$

where A is the anchoring strength coefficient, depending on the nematic-substrate interactions. The corresponding anchoring torque becomes

$$\Gamma_s(\varphi_s - \varphi_e) = \frac{d}{d\varphi_s} W_s = \frac{1}{2} A \sin[2(\varphi_s - \varphi_e)] \quad (2)$$

This elastic description of the anchoring assumes that, after the removal of the external torque, the director will go back to $\varphi_s = \varphi_e$. In reality, often the azimuthal anchoring depends strongly on the sample history. This anchoring memory phenomenon, described long ago^[2-4], is easily observable by the memorization of flow alignment patterns or surface walls^[5]. Recent experiments show, that under torque the easy axis itself can rotate in a viscous-like and irreversible (on torque removal) way. This "anchoring gliding" phenomenon, closely related to the anchoring memory, has been observed in both lyotropic^[6] and thermotropic^[7-10] nematics.

In the studies of the azimuthal anchoring, reported so far^[10-14], one applies an azimuthal torque on the surface director (magnetic^[15,16], electric^[9,12] or mechanical^[12,13,17]) and measures optically^[9,12-15,17] the deviation $\varphi_s - \varphi_e$. All techniques are limited to weak or moderately strong anchorings - it is difficult to create a large azimuthal torque, to control it and to measure $\varphi_s - \varphi_e$ while it is applied. Another difficulty arises for weak anchorings: they are, in general, strongly influenced by memory effects, e.g. by easy axis gliding. The separation of the gliding from the elastic director deviation is difficult and so far has not been thoroughly discussed.

Here we report the azimuthal anchoring strength and easy axis gliding of the nematic 5CB on weakly anisotropic substrate. We study the anchoring evolution at a time scale ranging from a few minutes up to a few months. We separate approximately the elastic and the viscous response and we obtain the gliding velocity as a function of the applied torque. We discuss the observed gliding times and nonlinear gliding viscosity.

EXPERIMENTAL

For this study we need a substrate with uniform azimuthal anchoring, weak intrinsic anisotropy and observable anchoring gliding. To achieve

this, we prepare a "sandwich" substrate: obliquely evaporated SiO is covered by a thin polyvinyl alcohol (PVA) film^[18]. The SiO layer gives a strong surface anisotropy^[19], the polymer screens it, making it weaker^[20]. The anchoring memory of PVA is relatively important, compared to the weak elastic contribution of the screened SiO^[21,22]. This memory is due mainly to an oriented nematic layer adsorption on PVA. Under torque the easy axis glides^[21,22], probably by slow desorption-readsorption.

The SiO is evaporated on flat glass plates at incidence angle 75° and thickness 2.5 nm. The PVA film is deposited on the SiO by slow withdrawal (0.05 mm/sec) from 2.5 % by weight solution of PVA in water. The plates are then dried for one hour at 110°C and used without further treatment. The measurement technique has been described elsewhere^[10,14]. A mechanical torque is applied on the substrate by twisting the cell at about 90° . Under torque, the surface director on the PVA deviates from the easy axis at angle $\delta = \phi_s - \phi_e$. The second substrate (counterplate) is chosen to have much stronger anchoring and negligible surface director deviation. Due to the symmetry of the uniformly twisted cell, a simple light transmission measurement^[10] gives δ , even when the sample is very thin and the wave guide regime of propagation is not valid. Advantages of this technique are its simplicity and the possibility to apply strong torques for long periods. A drawback is the difficulty to change the torque - the variation of the twist angle or the thickness strongly perturbs the weak anchoring on PVA. To avoid this problem, we construct our sample with counterplate made of weak curvature glass lens (aligned by SiO evaporation). In this way, the torque varies in large limits across the cell with the local thickness $d(r)$ (Figure 1), calculated from the known lens curvature.

As all weak anchorings, our substrates are very sensitive to flow alignment and other perturbations. To avoid these parasitic effects, we fill the cell with the nematic 5CB (4-n-pentyl-4'-cyanobiphenyl) in the isotropic state and at large gap ($>50\ \mu\text{m}$). Then, we cool slowly down to

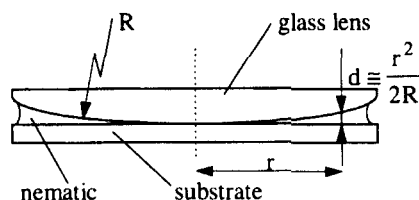


FIGURE 1 Cell geometry

room temperature. Observing the twist of the cell in wave guide regime, we adjust it to 90° by rotating the lens. In this way, we verify that $\varphi_e = 0$ on the PVA at the beginning of the experiment. Then, we carefully decrease the cell gap to zero, applying the twist torque

$$\Gamma_b = \frac{k_{22}}{d} \left(\frac{\pi}{2} - \varphi_s \right) \quad (3)$$

to the surface, where k_{22} is the twist elastic constant of 5CB and d is the local thickness (Figure 1). We start then our measurements of the surface director azimuth φ_s (Figure 2) as a function of d . Repeating periodically these measurements, we obtain φ_s also as a function of the time t .

On the time scale of our measurements (minutes), the φ_s relaxation is very rapid - the director follows the instantaneous torque equilibrium $\Gamma_b = \Gamma_s$. The time dependence of φ_e is much slower (see below). Approximately, we can suppose that the first curve on Figure 2 corresponds to $\varphi_e = 0$ and from the torque equilibrium we obtain $\Gamma_s(\varphi_s)$ (Figure 3). Γ_s has the expected Rapini-Papoular^[1] form. The anchoring strength, deduced from it, $A = 2.3 \cdot 10^{-6}$ N/m, corresponds to extrapolation length $L = k_{22}/A \cong 1.3 \mu\text{m}$, i.e. to weak anchoring.

On Figure 2 φ_s increases with the time. This can be due to a time dependent anchoring strength A in Equation (2) or, to easy axis gliding. Additional experiments show that the time variation of A , if any, is negligible. On the contrary, the gliding is easily observed (Figure 4) : when the torque is removed by increasing the cell gap, we observe directly that φ_e has glided in the thinnest part of the cell. We note also

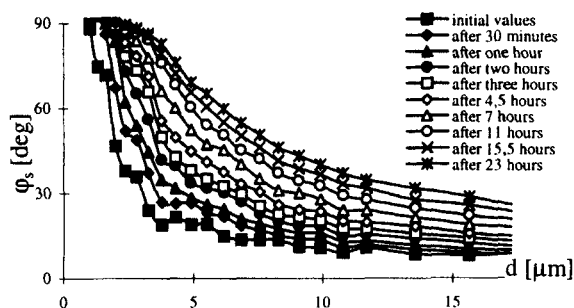


FIGURE 2 Surface director orientation φ_s as a function of the thickness and the time.

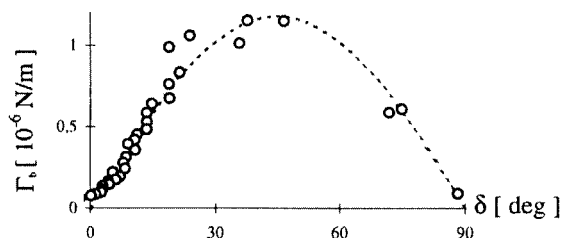


FIGURE 3 Relation between the torque and the elastic director $\delta = \varphi_s - \varphi_e$. The dashed line is a Rapini-Papoular fit with $l_e = 1.3 \mu\text{m}$.

that the gliding is much more visible on the PVA (Figure 4b), than on the bare SiO, where the anchoring is stronger.

In the following we suppose that the anchoring strength A does not vary in the time, and that the φ_s variation is due only to anchoring gliding. Then, from Equation (2), we calculate the curves $\varphi_e(t)$ at fixed thickness d (Figure 5). One sees that the characteristic gliding times τ_g vary in very large limits. At the beginning of the experiment $\tau_g \approx 2$ hours. At the end of it (after $t > 1$ month, not plotted on the figure) the exponential fit of $\varphi_e(t)$ gives $\tau_g \approx 200$ hours. These results are similar to the data recently reported for simpler SiO and rubbed PVA substrates^[23].

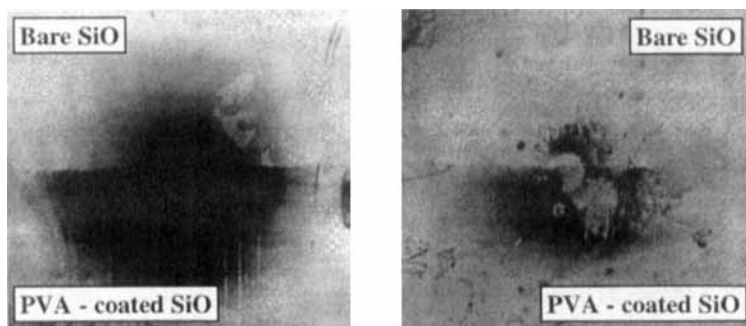
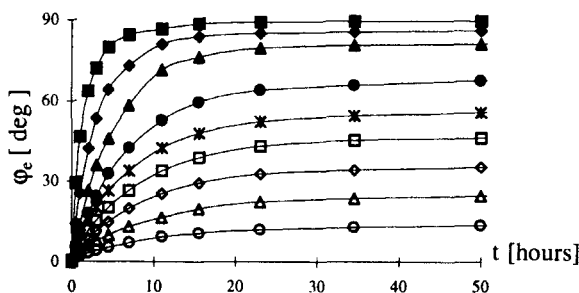


FIGURE 4 Microscopic image of the cell between crossed polarizers. (a) Elastic deviation under torque (the contact of the lens with the substrate lie on the edge of the PVA covered region) (b) On torque removal one observes that the easy axis has glided on PVA.

FIGURE 5 Time dependence of easy axis ϕ_e .

DISCUSSION

The characteristic times of gliding from Figure 5 depend, at fixed d , on the time dependent bulk torque Γ_b . Indeed, Γ_b changes along the curve $\phi_e(t)$ due to the gliding and the related twist variation. An useful way to present our data is to plot the gliding velocity $\dot{\phi}_e = d\phi_e / dt$ as a function of the torque. From the simplest viscous model of the gliding we expect

$$\Gamma_g = -\gamma_g \dot{\phi}_e \quad (4)$$

where Γ_g is the viscous gliding torque, and γ_g is a *gliding* viscosity. Neglecting the interaction of \mathbf{n}_e with the SiO, we assume $\Gamma_g = \Gamma_s$, i.e. the surface torque is equilibrated only by the viscous gliding torque.

Some typical experimental curves $\dot{\phi}_e(\Gamma_g)$ are presented on Figure 6. Each curve corresponds to a fixed thickness d and variable t . Two different gliding regimes are present on Figure 6, in disagreement with the linear response in Equation (4). At "short" times ($t < 10$ hours) $\dot{\phi}_e$ decreases rapidly at almost constant torque. This strange behavior is similar to solid friction, with friction coefficient rapidly decreasing above some threshold torque. However, our data show that there is no threshold torque - below the "threshold" $\dot{\phi}_e$ follows Equation (4). In this "slow" regime ($t \gg 10$ hours) the gliding viscosity coefficient is at least one order of magnitude higher.

The second disagreement of our data with the expected behavior is the non-universality of the curves on Figure 6. In fact, the curves $\dot{\phi}_e(\Gamma_g)$

for different d are similar, but not identical. This means, that the gliding velocity depends not only on the torque, but also on some additional, "hidden" parameter. This parameter can be φ_e (anisotropy of γ_g) or the time (hysteresis of γ_g). Our data are in better agreement with the hysteresis hypothesis. In fact, at $t=0$, when all the points have the same "clear" history, we find $\gamma_g=0.02 \text{ kg}\cdot\text{s}^{-1}$ independent from d or φ_e (Figure 6). This value of the gliding viscosity γ_g is several orders of magnitude higher than the expected surface viscosity γ_s , describing the friction of \mathbf{n}_s . In fact, both γ_g and γ_s have the dimension of surface viscosity and can be presented as $\gamma_i = \lambda_i \gamma$ ($i=s,g$), where γ is a nematic bulk viscosity and λ_i is some characteristic length. One expects $\lambda_s \sim 0.01 + 1 \mu\text{m}$ ^[24,25], while we obtain $\lambda_g \approx 0.2 \text{ m}$, obviously too large to have any physical sense. This confirms the necessity to distinguish γ_g and γ_s - while γ_s characterizes the rotation of \mathbf{n}_s , the gliding viscosity γ_g describes the much slower evolution of the surface layer itself.

So far, simpler behaviors have been reported, with gliding velocity linear^[9,23] or quadratic^[6] in Γ_b and without hysteresis. Two main differences with our experiment could explain this. First, in our case the applied torques are much stronger, going even up to anchoring breaking. One expects in this case stronger and, maybe, nonlinear gliding. The second difference is our complicated "sandwich" substrate, with anisotropic interaction SiO-PVA and, maybe, a superposition of two different gliding processes. Further experiments on simpler substrates could clarify this point.

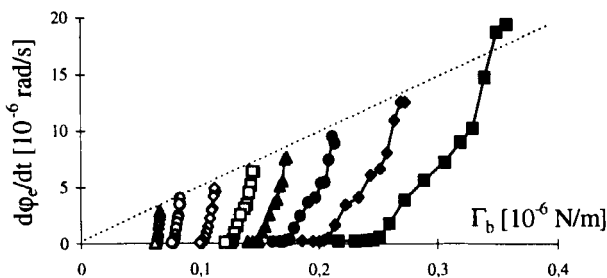


FIGURE 6 Gliding velocity as a function of the applied torque. Each curve is taken at fixed d and variable t . The dashed line is a fit to Equation (4) at $t=0$ and large thickness d .

To conclude, we present experimental results for the 5CB anchoring gliding under strong torques. We show that the gliding viscosity γ_g has a complicated, nonlinear behavior, and depends on the sample history. For better understanding of the gliding one needs new experiments, with simpler substrates, and new microscopic models for the evolution of the first nematic layer under torque.

Acknowledgements

We acknowledge fruitful discussions with G.Durand and financial support by European Community Grants ERBIC15CT960744 (Copernicus Program) and BRRT-CT97/5003 (SALC-NET Thematic Network).

References

- [1] R.Rapini and M.Papoular, *J.Phys.Coll.* (Paris), **30**, C4–54 (1969).
- [2] J.Cheng and G.D.Boyd, *Appl.Phys.Lett.*, **35**, 444 (1979).
- [3] H.Yokoyama, S.Kobayashi and H.Kamei, *J.Appl.Phys.*, **56**, 2645 (1984).
- [4] N.A.Clark, *Phys.Rev.Lett.*, **55**, 292 (1985).
- [5] M.Nobili, R.Barberi and G.Durand, *J.Phys.II*, **5**, 531 (1995).
- [6] E.A.Oliveira, A.M.Figueiredo Neto and G.Durand, *Phys.Rev.A*, **44**, R825 (1991).
- [7] T.Nose, S.Masuda and S.Sato, *Jpn.J.Appl.Phys.*, **1** (30), 3450 (1991).
- [8] Y.Sato, K.Sato and T.Uchida, *Jpn.J.Appl.Phys.*, **31**, L579 (1992).
- [9] V.P.Vorflusef, H.-S.Kitzerov and V.G.Chigrinov, *Appl.Phys.Lett.*, **70**, 3359 (1997).
- [10] R.Barberi, I.Dofov, M.Giocondo, M.Iovane, Ph.Martinot-Lagarde, D.Stoescu, S.Tonchev and L.V.Tsonev, *Eur.Phys.J.B*, **6**, 83 (1998).
- [11] S.Faetti, M.Gatti, V.Palleschi and T.J.Sluckin, *Phys.Rev.Lett.*, **55**, 1681 (1985).
- [12] S.Faetti, M.Nobili and A.Schirone, *Liq.Cryst.*, **10**, 95 (1991).
- [13] V.Sergan and G.Durand, *Liq.Cryst.*, **18**, 171 (1995).
- [14] E.Polossat and I.Dofov, *Mol.Cryst.Liq.Cryst.*, **282**, 223 (1996).
- [15] J.Sicart, *J.Phys.Lett.*, **37**, L-25 (1976).
- [16] S.Faetti, M.Gatti, V.Palleschi and A.Schirone, *Il Nuovo Cim.D*, **10**, 1313 (1988).
- [17] E.L.Wood, G.W.Bradberry, P.S.Cann and J.R.Sambles, *J.Appl.Phys.*, **82**, 2483 (1997).
- [18] S.Frunza, R.Moldovan, T.Beica, D.Stoescu and M.Tintaru, *Liq.Cryst.*, **14** (2), 293 (1993).
- [19] M.Monkade, Ph.Martinot-Lagarde, G.Durand and C.Granjean, *J.Phys.II* (Paris), **7**, 1577 (1997).
- [20] E.Dubois-Violette and P.G.de Gennes, *J.Phys.Lett.* (Paris), **36**, L255 (1975).
- [21] D.N.Stoescu, *Ph.D.These*, Paul Sabatier University – Toulouse, France, 1998.
- [22] D.N.Stoescu, Ph. Martinot-Lagarde and I.Dofov, accepted to *Mol.Cryst.Liq.Cryst.* (1999).
- [23] S.Faetti and M.Nobili, *Phys.Lett.A*, **217**, 133 (1996).
- [24] A.T.Mertelj and M.Copic, *Phys.Rev.Lett.*, **81** (26), 5844 (1998).
- [25] A.G.Petrov, A.Th.Ionescu, C.Versace and N.Scaramuzza, *Liq.Cryst.*, **19**, 169 (1995).